

Temperature Dependence of Charge-Transfer Fluorescence from Extended and U-shaped Donor–Bridge–Acceptor Systems in Glass-Forming Solvents[†]

Marijn Goes,[‡] Mattijs de Groot,[‡] Mattijs Koeberg,[‡] Jan W. Verhoeven,^{*,‡} Nigel R. Lokan,[§] Michael J. Shephard,[§] and Michael N. Paddon-Row^{*,§}

Laboratory of Organic Chemistry, IMC, University of Amsterdam, Nieuwe Achtergracht 129, 1018 WS Amsterdam, The Netherlands, and School of Chemistry, University of New South Wales, Sydney 2052, Australia

Received: July 2, 2001; In Final Form: October 2, 2001

The behavior is reported of three fluorescent D–bridge–A systems that display a fascinating temperature dependence in glass forming solvents over the temperature range between 77 and 293 K. In two of these systems, a rigid, saturated alkane bridge maintains an extended conformation, and as a result, the charge-transfer (CT) state is of giant dipolar nature. This causes the position of the CT fluorescence to be an extremely sensitive probe for the reorientation polarization of the surrounding medium. As a result, the thermochromism of the continuous CT fluorescence maximum in 2-methyltetrahydrofuran (MTHF) covers the full visible region. In the higher temperature domain (above ca. 145 K), this thermochromism can be quantitatively described via the Lippert–Mataga relation. At lower temperatures, solvent relaxation slows down sufficiently to detect exceptionally large dynamic Stokes shifts of the fluorescence maximum on time scales up to ≥ 40 ns. The third D–bridge–A system studied features a U-shaped ground state conformation. Remarkably, this system displays a significant thermochromic shift over a narrow temperature region around 175 K in the nonpolar methylcyclohexane (MCH) in which the other systems display only very minor thermochromism. In this U-shaped system therefore, one monitors the temperature dependence of an internal reorganization instead of a medium relaxation. Extensive ab initio calculations indicate that this internal reorganization must be related to an electrostatically driven conformational collapse of the U-shaped system in the CT state.

Introduction

Many (semi)rigid systems of the type D–bridge–A have been reported over the past decades in which an electron donor (D) and acceptor (A) are connected by a saturated alkane bridge with an extended conformation that maintains, at least in the ground state, a well defined orientation of D and A and a distance that prevents direct overlap of the D and A orbitals. In most such systems, intramolecular electron transfer has nevertheless been found to occur thermally or photochemically,^{1–4} if the combination of their structure and the solvating power of the medium makes this energetically feasible. This has, for example, allowed the study of the relative importance of through-bond (c.q. through-bridge) and through-medium interactions in mediating long-range electron transfer.

If a D–bridge–A system undergoes photoinduced electron transfer, this implies that a charge-transfer (CT) state is in principle the lowest singlet excited state. Radiative charge recombination is ubiquitous from states with a high CT character formed by electron transfer between D and A species under conditions that allow direct orbital overlap, i.e., from inter- or intramolecular “exciplexes”.⁵ For extended D–bridge–A systems devoid of direct orbital overlap, in which D and A are separated by two or more saturated carbon atoms, such radiative recombination has been reported only in a limited number of

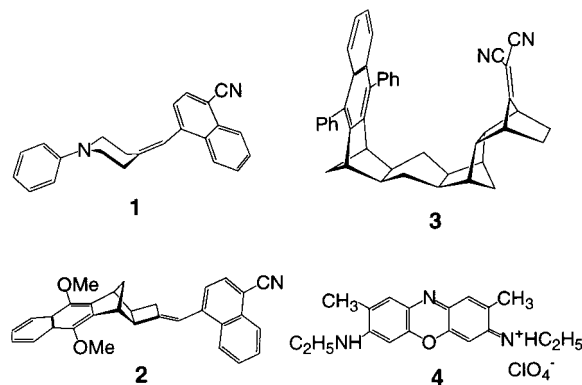


Figure 1. Structures of the donor–bridge–acceptor systems **1**, **2**, and **3** studied, as well as that of oxazine-4 (**4**) used for comparison.

cases^{6–15} and even then mostly with a (very) low quantum yield and in a limited solvent polarity range. There are, however, a few exceptions such as the extended D–bridge–A system **1** (see Figure 1), nicknamed Fluoroprobe (FP), and several closely related systems that have been reported to display bright and highly solvatochromic CT fluorescence with quantum yields in the 10–80% range over a wide range of solvent polarities.¹³ In these systems, an aniline type donor and an aryethylene acceptor are held in a rod-shaped conformation by a piperidine bridge. The extremely solvatochromic CT fluorescence of **1** and related systems has been studied in liquid solution,^{9,13,16–20} in polymeric matrices,^{21–29} on solid surfaces,³⁰ and even in the gas phase under supersonic jet cooled conditions.³¹ Because of the very

[†] Part of the special issue “Noboru Mataga Festschrift”.

* To whom correspondence should be addressed. Fax: 31-20-5255670. E-mail: jwv@science.uva.nl.

[‡] University of Amsterdam.

[§] University of New South Wales.

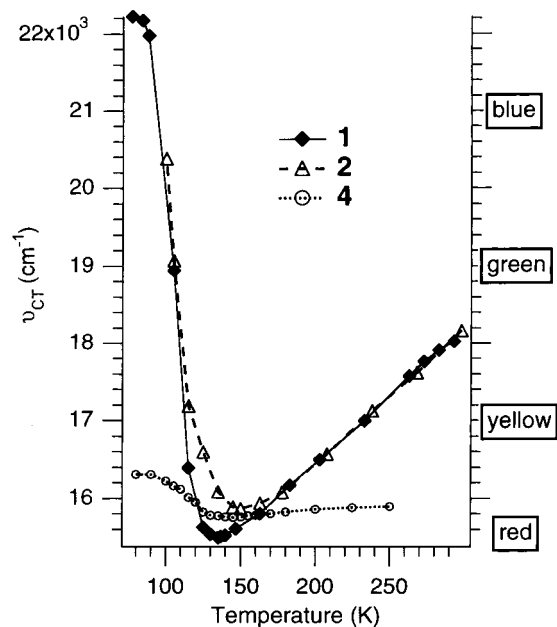


Figure 2. Thermochromic shift of the fluorescence for **1**, **2**, and **4** in MTHF.

large dipole moment of the CT fluorescent state inferred from various measurements,^{9,16,20} it has been assumed that the extended geometry of these molecules is maintained after charge separation and does not give way to the “crunch” of the electrostatic attraction that is known to lead to large conformational changes in more flexibly bridged systems.³¹

To confirm the conformational uniformity and extended nature of the CT fluorescent state of **1** under a variety of medium polarity and medium mobility conditions, we now compare the CT fluorescence of **1** with that of the newly synthesized system **2** (see Figure 1) over a wide temperature range in a glass-forming solvent. In both **2** and **1**, a π -electron donor/acceptor pair is held in an extended orientation by a saturated bridge providing a through-bond coupling path with an effective minimum length of three sigma bonds. However, the bridge structure of **2** is fully rigid and prohibits changes in the D/A distance, upon charge separation, that could in principle occur in **1** by, for example, a chair to (twist) boat ring flip of the central piperidine bridging unit. We will furthermore compare the temperature dependent behavior of system **1** in a glass-forming solvent with that of the U-shaped D-bridge-A system **3**. The latter was recently found¹⁵ to display detectable CT fluorescence, albeit with a much smaller quantum yield than **1**, and furthermore, evidence was presented that this CT fluorescence emerges from a state in which the donor-acceptor distance is considerably reduced as compared to the ground state under the influence of an electrostatically driven conformational collapse.

Results and Discussion

Thermochromism of 1 and 2 in MTHF. CT fluorescence maxima (in cm^{-1}) of **1** and **2** in 2-methyltetrahydrofuran (MTHF) over the 77–293 K temperature range are plotted in Figure 2. To better appreciate the extremely strong thermochromism of these CT fluorescences, we also have added to Figure 2 data for the well-known solvatochromic dye oxazine-4 (**4**) that has been studied earlier under these conditions by Görlach et al.³² Although **1**, **2**, and **4** behave similarly in a qualitative sense, the amplitude of the thermochromic frequency

changes is an order of magnitude larger for **1** and **2** than for **4**. As a result, the thermochromic shift of **1** (as well as that of **2**) in MTHF covers the whole visible region.

At 293 K, **1** displays a strong greenish yellow fluorescence in MTHF with a maximum located at 562 nm ($17\,800\text{ cm}^{-1}$) quite comparable to the behavior in tetrahydrofuran in which the fluorescence maximum of **1** was reported¹³ to be located at 571 nm with a quantum yield $\Phi = 16\%$ and a fluorescence lifetime $\tau = 8.7\text{ ns}$. Upon cooling of the MTHF solution, the CT fluorescence of **1** gradually shifts to the red with an average of $\sim 15\text{ cm}^{-1}/\text{K}$ until a bright red color is attained around 140 K. Upon further cooling, the red-shift first levels off and below 130 K changes to a very dramatic blue shift that in the 90–120 K region amounts to $-153\text{ cm}^{-1}/\text{K}$ and levels off again at lower temperatures. Qualitatively, this behavior can be readily understood along the same lines as put forward³² to describe the much less dramatic thermochromic effects displayed by **4** in MTHF. The excited state dipole moment of CT-fluorescent molecules induces reorientation (mainly rotational) of the solvent dipoles. This stabilizes the CT excited state and at the same time destabilizes the Franck-Condon ground state reached upon fluorescence. As long as the solvent reorientation occurs on a time scale which is fast, compared to the nanosecond fluorescence lifetime, the full red shift achievable by this process is present during most of the radiative process and is thus reflected in the position of the fluorescence maxima, measured by continuous emission spectroscopy as plotted in Figure 2. At room temperature, this condition is easily fulfilled as shown earlier by femtosecond time-resolved fluorescence measurements and molecular dynamics calculations for **1** in various solvents.^{18,19,33} From these investigations, it was firmly established that a time dependent Stokes shift only occurs over a time window of a few picoseconds after excitation as also expected from the typical dielectric solvent relaxation times under these conditions. As argued by others³² before, however, the solvent relaxation time of MTHF increases to nanoseconds upon cooling into the supercooled liquid region (i.e., below the melting point of $T_M = 135\text{ K}$) and rapidly increases further to seconds upon cooling to the glass transition point $T_G \approx 91\text{ K}$.

That below 135 K, in the temperature region where the thermochromicity levels off (see Figure 2), a sizable fraction of the overall fluorescence occurs from not fully relaxed states can easily be demonstrated from the fact that in this region the fluorescence displays a time dependent Stokes shift (see Figure 3) that extends over periods ranging from a few nanoseconds at 130 K to way over 40 ns (the maximum time window in which fluorescence can be detected) below 110 K.

In the high temperature region, where virtually all fluorescence occurs after full solvent relaxation, the thermochromic effect can in principle be described more quantitatively by the well-proven Lippert-Mataga expression (eq 1) that has been more widely employed for solvatochromic shifts.^{34,35} This expression accounts for the reorientation as well as the polarization of solvent molecules in terms of a solvent parameter Δf that depends (see eq 1A) on the bulk dielectric solvent permittivity (ϵ_s) and the refractive index (n):

$$v_{\text{CT}} = v_{\text{CT}}(0) - 2(\mu_{\text{CT}})^2 \Delta f / hc\rho^3 \quad (1)$$

$$\Delta f = (\epsilon_s - 1)/(2\epsilon_s + 1) - (n^2 - 1)/(4n^2 + 2) \quad (1A)$$

Equation 1 relates the fluorescence maximum observed (v_{CT}) and that extrapolated to the gas phase ($v_{\text{CT}}(0)$) with the dipole moment of the fluorescent state (μ_{CT}) and the effective radius

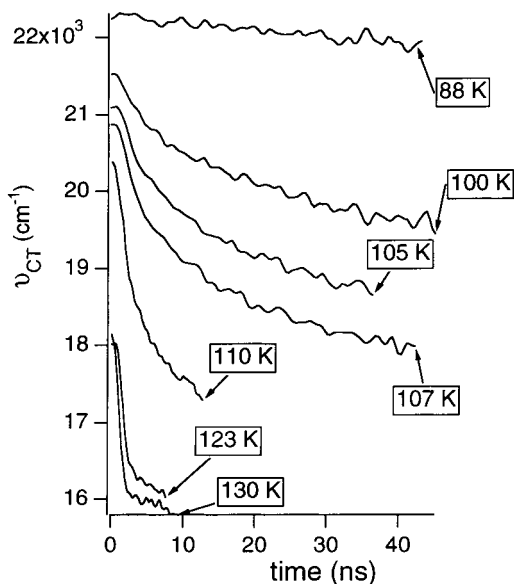


Figure 3. Dynamic Stokes shift of the fluorescence maximum at low temperatures for **1** in MTHF as observed with a streak camera after excitation at 337 nm (laser pulse width 600 ps fwhm).

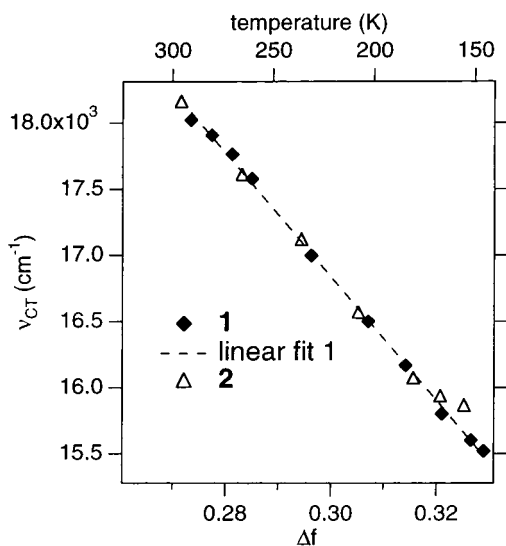


Figure 4. Lippert–Mataga plots of the thermochromic shift of the fluorescence for **1** and **2** in MTHF above 145 K. The regression line shown is that for **1**.

(ρ) of the solvent cavity in which the molecule fits. Although in solvatochromic studies Δf is varied by varying the solvent, in thermochromic studies such as those performed here, this parameter varies because both ϵ_s and n increase with decreasing temperature. This is in part because of the increased density but also because of the increased dipolar orientation of the solvent molecules with respect to the solute dipole as the counteracting thermal motions diminish upon cooling.³⁶

In Figure 4, we plot the ν_{CT} values of **1** and **2** as a function of the Δf increase brought about by cooling MTHF from 293 to 145 K. For this purpose, we took appropriate values of the refractive index³⁷ and the dielectric permittivity³⁸ from the literature.

Fairly linear plots are obtained down to ~ 145 K for **1** to ~ 160 K for **2**, whereas below this temperature, strong deviations start to occur because, as explained above, the emission no longer originates from a fully relaxed state. This becomes apparent for **2** at somewhat higher temperature (i.e., at lower

solvent viscosity) than for **1** simply because **1** has a longer fluorescence lifetime.

The slopes of the thermochromic Lippert–Mataga plots in Figure 4 are very similar for **1** and **2**, amounting to $-46\,000 \pm 2000$ cm^{-1} per Δf unit. Earlier, solvatochromic measurements for **1** gave a slope of the same order (i.e., $-30\,400$ cm^{-1}).⁹ According to eq 1, the slope of the Lippert–Mataga plot is governed by the excited-state dipole moment and the effective radius of the solvent cavity. Because the molecular dimensions of **1** and **2** are very comparable, so must be the volume of the effective solvent cavity they occupy. The actual value for the radius ρ of that cavity can be taken conveniently as 40% of the long axis of an ellipsoidal cavity in which these extended molecules fit. This gives $\rho = 5.4$ Å which then leads to $\mu_{CT} = 26.8$ D for both **1** and **2**. This value is well within the range of $\mu_{CT} = 27 \pm 2$ D reported earlier for **1** on the basis of various independent experimental techniques.^{9,13,16,20} Although the choice of an appropriate ρ value is always a bit arbitrary and influences the calculated μ_{CT} value, we stress that the comparison as presented here of the thermochromic shifts for **1** with those of the fully rigidly bridged **2** provides a very strong argument that **1** maintains its extended ground-state conformation also in the CT-fluorescent state at least in MTHF over the full temperature range investigated. In this connection, it is interesting to note that although the donor incorporated in **2** is somewhat weaker than that in **1**, the CT fluorescence maxima of these systems almost coincide. This implies that, probably because of the difference in donor, the internal reorganization energy in **2** must be larger than in **1** notwithstanding the higher bridge rigidity of the former!

The giant thermochromic effects displayed by **1** and **2** in MTHF (see Figure 2) also allowed us also to investigate further the nature of the excitation wavelength dependence of the oxazine-4 (**4**) fluorescence reported by Görlach et al.³² These investigators found that in the low-temperature region excitation with an excess energy ≥ 1000 cm^{-1} above the origin leads to a significant red shift of the fluorescence of **4**. They attributed this interesting phenomenon to local heating, caused by vibrational relaxation prior to the reorganization of the solvent shell. Because of their much stronger thermochromicity, this mechanism should lead to even more pronounced effects in the case of **1** and **2**. However, apart from a minor “red edge” effect of the opposite sign, no significant excitation wavelength dependence of the CT fluorescence maximum for **1** and **2** is observed over the whole temperature region investigated. We therefore are forced to conclude that the effect reported for **4** (and reproduced by us) must have another cause than the “local melting” proposed earlier. It should be noted that **4**, in contrast to **1** and **2**, is a cationic dye and that at low temperatures in MTHF it may be present in the form of variously composed and noninterconverting ion pairs with different excitation and emission spectra.

Thermochromism of 1 and 3 in Methylcyclohexane (MCH). Although the thermochromic data in MTHF provided proof for the extended nature of the CT fluorescent state of **1**, it should be realized that the electrostatic forces which try to diminish the donor–acceptor distance in the charge separated state of extended D–bridge–A molecules are strongly shielded by a dipolar solvent like MTHF. In earlier studies on (semi)-flexible D–bridge–A systems, evidence for strong electrostatically driven conformational changes (“harpooning”) was mostly obtained in nonpolar solvents with a low dielectric permittivity (i.e., in saturated alkanes)^{39,40} or even in the gas phase.³¹ We therefore deemed it important to investigate the thermochro-

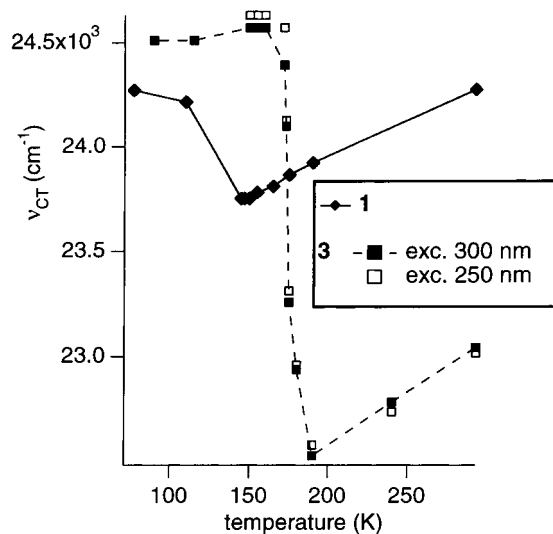


Figure 5. Thermochromic shift of the CT fluorescence maximum for **1** and **3** in MCH. For **3**, results employing two different excitation wavelengths (300 nm, filled squares, and 250 nm, open squares) are shown to demonstrate the absence of an effect of excess excitation energy (see text) on the sharp blue shift of **3** upon cooling below 190 K.

micity of **1** also in such a solvent for which we have chosen methylcyclohexane (MCH) because of its well established³⁸ glass-forming behavior ($T_G = 85$ K and $T_M = 146$ K). In addition to **1**, we also investigated in this solvent the behavior of the U-shaped D-bridge-A system **3**. The latter was recently found¹⁵ to display detectable CT fluorescence over a wide solvent polarity range, albeit with a quantum yield of only about 1%, i.e., much smaller than that of **1**. From preliminary ab initio calculations on a model of **3**, it was proposed that, upon photoinduced charge separation, the electrostatic forces in the CT state enforce a considerable reduction of the center-to-center D/A distance.^{15,41} This conformational collapse is largely brought about by pyramidalisation of the acceptor radical anion, with additional bending in the other parts (donor radical cation and bridge) of the molecule.

In Figure 5, we now compare the thermochromic behavior of **1** and **3** in MCH over the 77–293 K temperature range. In contrast to the situation in MTHF (see Figure 2), system **1** displays only a very minor thermochromism in MCH. This is, of course, fully in line with the explanation given for the huge thermochromic effects observed in MTHF in terms of rotational relaxation of the solvent dipoles around the giant dipolar CT state of **1**. The molecular dipole moment of MCH (calculated in AM1 to be 0.01 D) is negligible, compared to that of MTHF (calculated in AM1 to be 1.67 D, and measured³⁸ to be 1.38 D), whereas also the molecular polarizability tensor of MCH is expected to be close to spherical. As a result, the maximum amplitude of the thermochromic effect for **1** over the temperature range studied amounts only to 520 cm^{-1} in MCH, compared to 6720 cm^{-1} in MTHF. The lack of significant thermochromism for **1** in MCH again indicates that also, in MCH, **1** retains its extended conformation in the CT fluorescent state even though the electrostatic forces that try to reduce the D/A distance are stronger in MCH than in MTHF. More convincing evidence for this arises by comparison with the thermochromic behavior of **3** in MCH (see Figure 5). Upon cooling from 293 K, the CT fluorescence of **3** initially undergoes a modest red shift of a magnitude comparable to that observed for **1**. As explained before, this can readily be attributed to the (in this case slight)

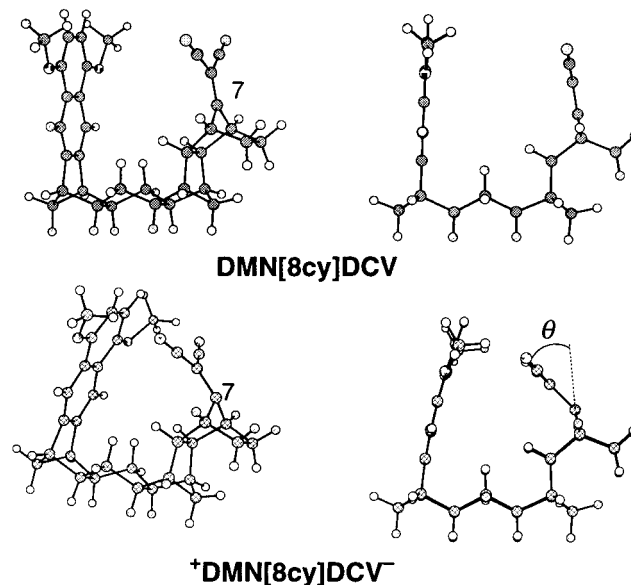


Figure 6. Calculated equilibrium conformation of **DMN[8cy]DCV** in the ground state (top) and in the CT state (bottom).

increase of the solvent Δf value, mainly as a result of the increased density. For **1**, this modest red shift pertains down to temperatures at which we enter the supercooled liquid regime ($T_M = 146$ K)⁴² and is then substituted by an equally modest blue shift upon further cooling into the glass-forming region ($T_G = 85$ K). However, in the 190–170 K region, the CT fluorescence of **3** undergoes a sharp (reversible) blue shift of about 2100 cm^{-1} and then levels off again.

This sudden jump in the emission frequency can be understood if we assume that it is related to a (partial) freezing-out of the electrostatically driven conformational change that diminishes the D/A distance in the CT state of **3**.

That the origin of the hypsochromic shift of 2100 cm^{-1} is probably due to the CT state of **3** adopting different geometries in MCH depending on the temperature receives support from a combination of gas-phase UHF and DFT calculations on a closely related model **DMN[8cy]DCV**. This model (see Figure 6) contains the same 1,1-dicyanovinyl (DCV) acceptor as **3** and the same 8-bond bridge ([8cy]), but the 1,4-diphenyl-naphthalene donor unit of **3** is substituted by a 1,4-dimethoxynaphthalene (DMN) donor unit. Geometry optimizations of **DMN[8cy]DCV** and its singlet CT state were carried out under C_s symmetry constraint using respectively the HF/6-31G(d) and UHF/3-21G methods and the resulting conformations are shown in Figure 6. It has been demonstrated that the UHF/3-21G level of theory gives satisfactory optimized geometries of CT states.^{41,43} In the ground state of **DMN[8cy]DCV**, both the DMN moiety and the DCV group are essentially planar. This is not the case, however, in the CT state, ${}^+\text{DMN[8cy]DCV}^-$: The DCV⁻ group is quite strongly pyramidalized about C7, with a pyramidalization angle, θ , of 34.6° . The ${}^+\text{DMN}$ radical cation group and the norbornylogous bridge are also slightly distorted, compared to their ground-state geometries. The distortions experienced in the CT state combine to bring the ${}^+\text{DMN}$ and DCV⁻ groups into close proximity, with the driving force being electrostatic stabilization in origin.

A measure of the extent of contraction of the DMN–DCV distance, brought about by charge separation, is the change in the magnitude of the distance between the centroid of the two nitrogen atoms in the DCV group and the centroid of the DMN ring. In the ground state, this distance is 6.15 \AA , whereas in the

CT state, it shortens to only 3.94 Å. If the DCV[−] group in the CT state were forced to be planar, then the centroid-centroid distance is 5.63 Å.

We assume that, in MCH below 170 K, the solvent somehow prevents the DCV[−] radical anion group from realizing its preferred pyramidalized structure, upon formation of the CT state of **3**. This is reasonable on energetic grounds because the pyramidalization potential of the norbornene–DCV radical anion by itself is quite weak, amounting to only ca. 14 kJ mol^{−1}, for $\theta = 40^\circ$ out-of-plane distortion.

We shall refer to the model ⁺DMN[8cy]DCV[−] CT structure that possesses the optimal (gas phase) pyramidalized DCV[−] group as the relaxed CT state and the modified structure, possessing a planar DCV[−] group, as the unrelaxed CT state.

The (gas phase) energy difference between the relaxed and unrelaxed CT states of ⁺DMN[8cy]DCV was calculated using time-dependent density functional theory (TD-DFT).^{44–48} This level of theory is being successfully used to calculate various properties of CT states of the type discussed here.⁴⁹ Using the B3P86 functional, as implemented in Gaussian 98,⁵⁰ and the 6-311G(d) basis set, the unrelaxed structure was calculated to lie 3439 cm^{−1} higher in energy than the relaxed structure. This is more than the actual thermochromic shift of 2100 cm^{−1} observed for **3** in MCH (see Figure 5), which suggests that the conformational collapse cannot be frozen out completely.

In this connection, it is important to point out that, at the UHF/3-21G level of theory, the CT state possessing a planar DCV radical anion group is not a minimum energy structure at all; the energy of the CT state rises monotonically with decreasing degree of pyramidalization and continues to rise when the direction of pyramidalization becomes reversed, so that the DCV entity points away from the ⁺DMN group. Thus, it is likely that some degree of pyramidalization will still take place in low-temperature methylcyclohexane. Furthermore, because the calculated energy gain of 3439 cm^{−1} for the geometry relaxation in the gas phase is largely electrostatic in nature, this gain will certainly be reduced to some degree by the shielding action of the surrounding MCH shell (with a bulk dielectric permittivity of $\epsilon_s \approx 2$).

It is important to point out that at 170 K MCH is still an (undercooled) liquid and that at first sight it is quite amazing that the barrierless conformational collapse of the CT state can be impeded at all under these conditions. That implies that around 180 K the rate of the conformational change takes place on a time scale comparable with the fluorescence lifetime which is about 25 ns. If the rate would be determined by an internal conformational barrier, and shows Arrhenius type behavior, the activation energy to cross that barrier should amount to about 3.5 kcal/mol to reach a crossing time of 25 ns at 180 K. However, the thermochromic jump observed occurs in a much too narrow temperature region to be explained by an Arrhenius-type behavior. It therefore is relevant to note that below 208 K the viscosity of MCH is known⁵¹ to increase in a non-Arrhenius fashion. This has been interpreted to imply that the rotational freedom of the solvent becomes restricted to rotation around a single axis, which may imply that pushing aside MCH solvent molecules by, for example, rotation around their short axis during the conformational collapse of the CT state in **3** also becomes impossible below a sharply defined temperature in the region in which MCH displays such non-Arrhenius viscosity behavior.

In conclusion, the thermochromicity data for **3** in MCH show that it is possible to restrict, at least in part, the electrostatically driven conformational collapse depicted in Figure 6, even though

the gas-phase structure of the CT state of **3**, possessing a planar DCV geometry, is not a minimum energy structure. An eventual conformational collapse of the extended CT state in **1** requires much larger motions and especially also involves internal barriers related to, for example, a chair to (twist) boat ring flip of the central piperidine bridge. The occurrence of such a collapse for **1** and related CT fluorescent probes can now be excluded with confidence in both dipolar (MTHF) and saturated alkane (MCH) media. This allows the interpretation of the temperature and medium-dependent shifts in the CT fluorescence of **1** and related probes as being due to “external” factors in the absence of large internal changes.

The absence of local melting/softening of the solvent shell by excess excitation energy already noted for **1** and **2** in MTHF is further supported by the behavior of **3**. Notwithstanding the extremely sharply defined temperature range in which “switching” between CT emission of **3** in MCH from two conformations occurs, no significant effects of the excitation wavelength on this are observed (see Figure 5). In fact, excitation at 300 nm instead of at 250 nm, which implies a decrease of the excess energy from about 0.83 eV to nearly zero, induces a very small red shift (i.e., a typical “red edge” effect) instead of a blue shift in the low-temperature region.

Experimental Section

Materials. Spectroscopic grade 2-methyltetrahydrofuran (Aldrich) was distilled over sodium wire and dried over molsieves. Spectroscopic grade methylcyclohexane (Aldrich) was purified over activated silica. The syntheses of **1**⁹ and **3**¹⁵ were described previously. Oxazine **4** was obtained from Radiant Dyes. The synthesis of **2** is described in the Supporting Information.

Measurements. All temperature-dependent measurements were carried out using degassed samples in a nitrogen cooled optical cryostat (DN1704, Oxford Instruments) with controller (ITC4, Oxford Instruments). Steady-state UV/vis emission spectra were recorded on a SPEX Fluorolog III equipped with two double monochromators (excitation and emission). The detector was a Peltier-cooled R636-10 (Hamamatsu) photomultiplier tube. To separate the rather weak fluorescence of **3** from impurity luminescence of the MCH solvent at low temperatures as well as from the phosphorescence of **3** itself, that set on when the solvent rigidifies, time gated fluorescence detection was used. For excitation, a Q-switched Nd:YAG laser (Infinity, Coherent) at 10 Hz was employed. In this system, the frequency tripled output (355 nm) of the YAG laser pumps a broad-band optical parametric oscillator, and the signal beam of this is frequency doubled to obtain tunable pulses in the near UV (~1.5 mJ/pulse, 2 ns fwhm, 220–350 nm). The fluorescence emerging from the sample is collected via a spectrograph (SpectraPro-150, Acton) which disperses it on a gated intensified CCD camera (ICCD-576-G/RB-EM, Princeton Instruments). A gate-width of 30 ns was used, starting 25 ns after the laser pulse. Thereby, prompt local fluorescence and the long-lived phosphorescence were excluded from the signal. Time-resolved fluorescence measurements of the dynamic Stokes shift of **1** (see Figure 3) were performed using a streak camera system (Hamamatsu, details described elsewhere⁵²). For excitation, both the above-mentioned Nd:YAG laser and a nitrogen laser (MSG400, LTB, 337 nm, fwhm \approx 0.6 ns, 10 Hz) were used. The time-resolved shift of the fluorescence maximum was obtained from the fit of the spectral information every 0.4 ns to a skewed Gaussian function.⁵³

Acknowledgment. The authors like to thank The Netherlands Organization for Scientific Research (NWO) and the

Australian Research Council (ARC) for their financial support. MNP-R also thanks the ARC for the award of a Senior Research Fellowship. We acknowledge the New South Wales Centre for Parallel Computing and the ac3 facility for generous allocation of computer time.

Supporting Information Available: Experimental details (text and scheme) for the synthesis of **2** as well as Cartesian coordinates for the RHF/6-31G(d) optimized geometry (lowest energy conformation) of **DMN[8cy]DCV** in its ground state and the UHF/3-21G optimized geometry of the ⁺**DMN[8cy]DCV**⁻CT state. This material is available free of charge via the Internet at <http://pubs.acs.org>.

References and Notes

- Closs, G. L.; Miller, J. R. *Science* **1988**, *240*, 440.
- Wasielowski, M. R. *Chem. Rev.* **1992**, *92*, 435.
- Verhoeven, J. W. In *Advances in Chemical Physics, Electron Transfer- From Isolated Molecules to Biomolecules, Part One*; Jortner, J., Bixon, M., Eds.; John Wiley & Sons: New York, 1999; Vol. 106, p 603.
- Paddon-Row, M. N. In *Electron-Transfer In Chemistry*; Balzani, V., Ed.; Wiley-VCH: Weinheim, Germany, 2001; Vol. 3, part 2, Chapter 1, p 179.
- Gordon, M.; Ware, W. R., Eds.; *The Exciplex*; Academic Press: New York, 1975.
- Dekkers, A. W. J. D.; Verhoeven, J. W.; Speckamp, W. N. *Tetrahedron* **1973**, *29*, 1691.
- Pasman, P.; Verhoeven, J. W.; deBoer, T. J. *Chem. Phys. Lett.* **1978**, *59*, 381.
- Pasman, P.; Rob, F.; Verhoeven, J. W. *J. Am. Chem. Soc.* **1982**, *104*, 5127.
- Mes, G. F.; deJong, B.; vanRamesdonk, H. J.; Verhoeven, J. W.; Warman, J. M.; DeHaas, M. P.; HorsmanVanDeDool, L. E. W. *J. Am. Chem. Soc.* **1984**, *106*, 6524.
- Hush, N. S.; Paddon-Row, M. N.; Cotsaris, E.; Oevering, H.; Verhoeven, J. W.; Heppener, M. *Chem. Phys. Lett.* **1985**, *117*, 8.
- Oevering, H.; Paddon-Row, M. N.; Heppener, M.; Oliver, A. M.; Cotsaris, E.; Verhoeven, J. W.; Hush, N. S. *J. Am. Chem. Soc.* **1987**, *109*, 3258.
- Oevering, H.; Verhoeven, J. W.; Paddon-Row, M. N.; Warman, J. M. *Tetrahedron* **1989**, *45*, 4751.
- Hermant, R. M.; Bakker, N. A. C.; Scherer, T.; Krijnen, B.; Verhoeven, J. W. *J. Am. Chem. Soc.* **1990**, *112*, 1214.
- Oliver, A. M.; Paddon-Row, M. N.; Kroon, J.; Verhoeven, J. W. *Chem. Phys. Lett.* **1992**, *191*, 371.
- Koeberg, M.; deGroot, M.; Verhoeven, J. W.; Lokan, N. R.; Shephard, M. J.; Paddon-Row, M. N. *J. Phys. Chem. A* **2001**, *105*, 3417.
- Rodrigues, S. V.; Maiti, A. K.; Reis, H.; Baumann, W. *Mol. Phys.* **1992**, *75*, 953.
- Scherer, T.; Hielkema, W.; Krijnen, B.; Hermant, R. M.; Eijckelhoff, C.; Kerkhof, F.; Ng, A. K. F.; Verleg, R.; Tol, E. B. v. d.; Brouwer, A. M.; Verhoeven, J. W. *Recl. Trav. Chim. Pays-Bas* **1993**, *112*, 535.
- Middelhoek, E. R.; Vermeulen, P.; Verhoeven, J. W.; Glasbeek, M. *Chem. Phys. Lett.* **1995**, *198*, 373.
- Middelhoek, E. R.; Zhang, H.; Verhoeven, J. W.; Glasbeek, M. *Chem. Phys.* **1996**, *211*, 489.
- Smirnov, S. N.; Braun, C. L. *Rev. Sci. Instr.* **1998**, *69*, 2875.
- vanRamesdonk, H. J.; Vos, M.; Verhoeven, J. W.; Möhlman, G. R.; Tissink, N. A.; Meesen, A. W. *Polymer* **1987**, *28*, 951.
- Jenneskens, L. W.; vanRamesdonk, H. J.; Verhey, H. J.; vanHouwelingen, G. D. B.; Verhoeven, J. W. *Recl. Trav. Chim. Pays-Bas* **1989**, *108*, 453.
- Jenneskens, L. W.; Verhey, H. J.; vanRamesdonk, H. J.; Witteveen, A. J.; Verhoeven, J. W. *Macromolecules* **1991**, *24*, 4038.
- Jenneskens, L. W.; Verhey, H. J.; vanRamesdonk, H. J.; Verhoeven, J. W.; vanMalssen, K. F.; Schenk, H. *Recl. Trav. Chim. Pays-Bas* **1992**, *111*, 507.
- Verhey, H. J.; Gebben, B.; Hofstraat, J. W.; Verhoeven, J. W. *J. Polym. Sci.: Part A: Polym. Chem.* **1995**, *33*, 399.
- Hofstraat, J. W.; Verhey, H. J.; Verhoeven, J. W.; Kumke, M. U.; Li, G.; Hemmingsen, S. L.; McGown, L. B. *Polymer* **1997**, *38*, 2899.
- Verhey, H. J.; vanderVen, L. G. J.; Bekker, C. H. W.; Hofstraat, J. W.; Verhoeven, J. W. *Polymer* **1997**, *38*, 4491.
- Warman, J. M.; Abellon, R. D.; Verhey, H. J.; Verhoeven, J. W.; Hofstraat, J. W. *J. Phys. Chem. B* **1997**, *25*, 4913.
- Warman, J. M.; Abellon, R. D.; Luthjens, L. H.; Suykerbuyk, J. S.; Verheij, H. J.; Verhoeven, J. W. *Nuclear Instrum. Methods Phys. Res. B* **1999**, *151*, 361.
- Bartels, M. J.; Koeberg, M.; Verhoeven, J. W. *Eur. J. Org. Chem.* **1999**, 2391.
- Wegewijs, B.; Verhoeven, J. W. In *Advances in Chemical Physics, Electron Transfer- From Isolated Molecules to Biomolecules, Part One*; Jortner, J., Bixon, M., Eds.; John Wiley & Sons: New York, 1999; Vol. 106, pp 221.
- Görlach, E.; Gygax, H.; Lubini, P.; Wild, U. P. *Chem. Phys.* **1995**, *194*, 185.
- Brown, R.; Middelhoek, R.; Glasbeek, M. *J. Chem. Phys.* **1999**, *111*, 3616.
- Mataga, N.; Kaifu, Y.; Koizumi, M. *Bull. Chem. Soc. Jpn.* **1955**, *28*, 690.
- Lippert, E. *Z. Naturforsch. A* **1955**, *10*, 541.
- Suppan, P.; Tsiamis, C. *J. Chem. Soc., Faraday Trans. 2* **1981**, *77*, 1553.
- Timmermans, J. *Physico-Chemical Constants of Pure Organic Compounds*; Elsevier: Amsterdam, The Netherlands, 1986; Vol. 2.
- Streck, C.; Richert, R. *Ber. Bunsen-Ges. Phys. Chem.* **1994**, *98*, 619.
- Lauterlager, X. Y.; Bartels, M. J.; Piet, J. J.; Warman, J. M.; Verhoeven, J. W.; Brouwer, A. M. *Eur. J. Org. Chem.* **1998**, 2467, 7.
- Bleisteiner, B.; Marian, T.; Schneider, S.; Brouwer, A. M.; Verhoeven, J. W. *Phys. Chem. Chem. Phys.* **2001**, *3*, 2070.
- Shephard, M. J.; Paddon-Row, M. N. *J. Phys. Chem. A* **2000**, *104*, 11628.
- Sare, J. M.; Sare, E. J.; Angell, C. A. *J. Phys. Chem.* **1978**, *82*, 2622.
- Shephard, M. J.; Paddon-Row, M. N. *J. Phys. Chem. A* **1999**, *103*, 3347.
- Ahlich, R.; Bär, M.; Häser, M.; Horn, H.; Kölmel, C. *Chem. Phys. Lett.* **1989**, 162.
- Bauernschmitt, R.; Ahlich, R. *Chem. Phys. Lett.* **1996**, *256*, 454.
- Bauernschmitt, R.; Häser, M.; Treutler, O.; Ahlich, R. *Chem. Phys. Lett.* **1997**, *264*, 573.
- Handy, N. C.; Tozer, D. J. *J. Comput. Chem.* **1999**, *20*, 106.
- Wiberg, K. B.; Stratmann, R. E.; Frisch, M. J. *Chem. Phys. Lett.* **1998**, *297*, 60.
- Paddon-Row, M. N.; Shephard, M. J. *J. Am. Chem. Soc.* **2001**, submitted.
- Frisch, M. J.; Trucks, G. W.; Schlegel, H. B.; Scuseria, G. E.; Robb, M. A.; Cheeseman, J. R.; Zakrzewski, V. G.; Montgomery, J. A., Jr.; Stratmann, R. E.; Burant, J. C.; Dapprich, S.; Millam, J. M.; Daniels, A. D.; Kudin, K. N.; Strain, M. C.; Farkas, O.; Tomasi, J.; Barone, V.; Cossi, M.; Cammi, R.; Mennucci, B.; Pomelli, C.; Adamo, C.; Clifford, S.; Ochterski, J.; Petersson, G. A.; Ayala, P. Y.; Cui, Q.; Morokuma, K.; Malick, D. K.; Rabuck, A. D.; Raghavachari, K.; Foresman, J. B.; Cioslowski, J.; Ortiz, J. V.; Stefanov, B. B.; Liu, G.; Liashenko, A.; Piskorz, P.; Komaromi, I.; Gomperts, R.; Martin, R. L.; Fox, D. J.; Keith, T.; Al-Laham, M. A.; Peng, C. Y.; Nanayakkara, A.; Gonzalez, C.; Challacombe, M.; Gill, P. M. W.; Johnson, B. G.; Chen, W.; Wong, M. W.; Andres, J. L.; Head-Gordon, M.; Replogle, E. S.; Pople, J. A. *Gaussian 98*; Gaussian, Inc.: Pittsburgh, PA, 1998.
- Carpenter, M. R.; Davies, D. B.; Matheson, A. J. *J. Chem. Phys.* **1967**, *46*, 2451.
- Lauterlager, X. Y.; vanStokkum, I. H. M.; vanRamesdonk, H. J.; Brouwer, A. M.; Verhoeven, J. W. *J. Phys. Chem. A* **1999**, *103*, 653.
- Marcus, R. A. *J. Phys. Chem.* **1989**, *93*, 3078.